

Can Indian Ocean SST anomalies influence South American rainfall?

Andréa S. Taschetto · Tércio Ambrizzi

Received: 14 November 2010 / Accepted: 9 August 2011 / Published online: 20 August 2011
© Springer-Verlag 2011

Abstract In this study we examine the impact of Indian Ocean sea surface temperature (SST) variability on South American circulation using observations and a suite of numerical experiments forced by a combination of Indian and Pacific SST anomalies. Previous studies have shown that the Indian Ocean Dipole (IOD) mode can affect climate over remote regions across the globe, including over South America. Here we show that such a link exists not only with the IOD, but also with the Indian Ocean basin-wide warming (IOBW). The IOBW, a response to El Niño events, tends to reinforce the South American anomalous circulation in March-to-May associated with the warm events in the Pacific. This leads to increased rainfall in the La Plata basin and decreased rainfall over the northern regions of the continent. In addition, the IOBW is suggested to be an important factor for modulating the persistence of dry conditions over northeastern South America during austral autumn. The link between the IOBW and South American climate occurs via alterations of the Walker circulation pattern and through a mid-latitude wave-train teleconnection.

Keywords South American climate · Indian Ocean variability · Northeast Brazil · Southern hemisphere teleconnections

1 Introduction

The tropical Indian Ocean impacts climate around the world via two primary patterns of variability: (1) a uniform signal throughout the basin (Chambers et al. 1999) and (2) the Indian Ocean Dipole (IOD; Saji et al. 1999). In the past decade, the IOD has dominated the attention of scientists, presumably due to the ongoing debate over the genesis of this phenomenon. Whether the IOD is an oscillatory mode of intrinsic variability of the Indian Ocean that is independent of ENSO is still under debate (e.g. Baquero-Bernal et al. 2002; Dommenges and Latif 2002; Fischer et al. 2005; Behera et al. 2006). Regardless of the debate on the origin of the IOD, previous studies have shown that after the SST dipole is formed in the Indian Ocean, it has the potential to modulate the monsoon regime over South Asia (e.g. Ashok et al. 2001), precipitation over eastern Africa (e.g. Clark et al. 2003; Ummenhofer et al. 2009a) and rainfall over southeastern Australia (e.g. Ummenhofer et al. 2009b; Cai et al. 2009).

The impacts of the IOD onto South American climate have been less studied, possibly due to the relatively remote location of the forcing. A previous study from Saji et al. (2005) has reported a remote teleconnection pattern via a stationary Rossby wave train that emanates from the Indian Ocean sector towards South America during austral spring. This teleconnection pattern affects the remote circulation over the continent and induces an anomalous dipole pattern in rainfall, with decreased precipitation in the north and enhanced rainfall in the southern regions (Chan et al. 2008).

The Southern Hemisphere climate impacts associated with the leading pattern of Indian Ocean SST variability has received relatively less attention than the IOD. The leading pattern is a uniform basin wide signal that accounts

A. S. Taschetto (✉)
Climate Change Research Centre, University of New South
Wales, Sydney, NSW 2052, Australia
e-mail: a.taschetto@unsw.edu.au

T. Ambrizzi
Department of Atmospheric Sciences, University of São Paulo,
São Paulo, Brazil

for approximately one-quarter of the monthly tropical Indian Ocean SST variability (Fig. 1). The positive phase of this pattern, known as the Indian Ocean basin-wide warming (IOBW), is a remote response to El Niño events (Klein et al. 1999). The IOBW exhibits a preference for peaking from December to April, as shown by the monthly standard deviation of the leading principal component defined here as the IOBW index (Fig. 2a). On the other hand, the IOD appears strong between June and November (Fig. 2a). Figure 1a also shows that when the IOBW peaks, El Niño experiences a sharply decay, reaching minimum variations in March–April.

The IOBW index reveals a periodicity of approximately 4 years associated with El Niño events (Fig. 1c). The relationship between the Indian Ocean and the El Niño–Southern Oscillation (ENSO) is clearly detected in a simple correlation analysis shown in Fig. 2b. The IOBW is highly correlated with Niño3 index December–March, with a maximum coefficient of 0.79 in January. When the IOBW–ENSO relationship weakens, correlations between the IOD and Niño3 strengthen, reaching a maximum coefficient of 0.66 in October (Fig. 2b).

The dynamical/thermodynamical link between ENSO and the IOBW can be explained as follows. During the development of El Niño events (i.e. from June to November), the eastern Indian Ocean is relatively cold, essentially in a positive IOD state. With the arrival of the Australian monsoon, the trade winds relax, becoming

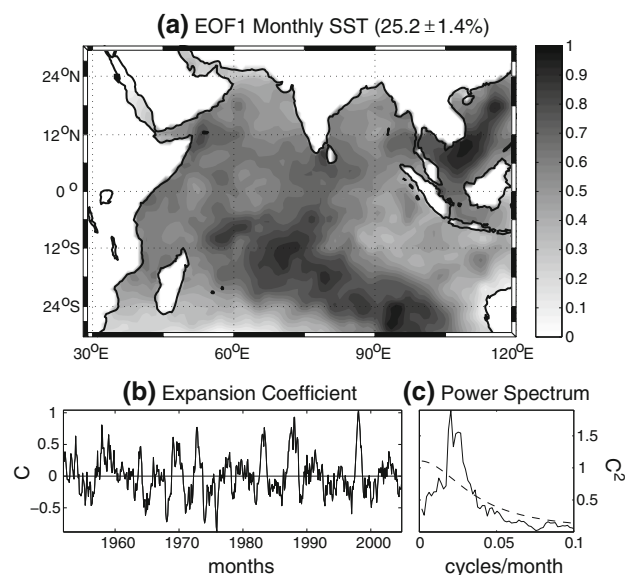


Fig. 1 **a** Leading EOF pattern of the tropical Indian Ocean, accounting for approximately 25% of the explained variance of the monthly SST anomalies from 1950 to 2006. Contour intervals are 0.05. **b** Associated time series of the expansion coefficient, used as the Indian Ocean basin-wide warming (IOBW) index. **c** Power spectrum via Multi-Taper Method associated with the IOBW index. A peak of 4-years period is significant at the 0.05 level based on a *F* test

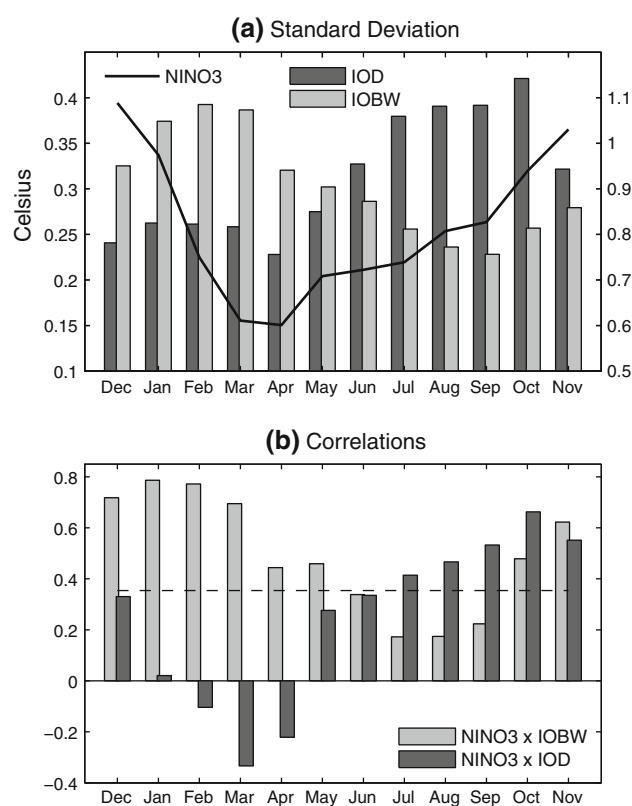


Fig. 2 **a** Month-by-month standard deviation of the IOBW (light gray bars), IOD (dark gray bars) and Niño3 index (black line). **b** Correlation coefficient between Niño3 index and the IOBW (light gray bars) and the IOD (dark gray bars). The dashed line indicates correlations significant at the 0.01 level

westerly. This weakens the oceanic upwelling and reduces surface cooling via changes in latent heat flux. In November–December, when El Niño is mature, it generates subsidence and an anticyclonic wind stress anomaly over the eastern Indian Ocean via an anomalous Walker circulation. This reduces convection, the formation of clouds, and enhances the net heat flux into the ocean (Klein et al. 1999), thus rapidly warming the eastern Indian Ocean basin. The anomalous wind stress decreases the wind speed and leads to oceanic downwelling Rossby waves (Chambers et al. 1999) that propagate to the west, creating the uniform warming of the Indian Ocean 3–4 months after the peak of El Niños (Lau and Nath 2003). A thorough review of the dynamics of the IOBW can be found in Schott et al. (2009).

The effect of the IOBW onto the Southern Hemisphere climate has been overlooked in the literature presumably due to two reasons. Firstly, it co-occurs with El Niño events that are larger in amplitude and extension, so it is justifiable that scientists focus primarily on the impacts of the relatively prominent warm Pacific episodes. Secondly, the IOBW is not an independent mode of variability in a physical sense, i.e. it is an

indirect effect of El Niño events. Nevertheless, this should not suggest an indirect El Niño effect cannot influence the local and/or the remote atmospheric circulation. For instance, previous studies have found that the IOBW can significantly impact the Northern Hemisphere climate. Annamalai et al. (2005) and Xie et al. (2009) have reported the influence of the tropical Indian Ocean warming onto South Asian monsoon and western Pacific climate. Yang et al. (2009) has shown that the uniform warming of the Indian Ocean can actually produce a significant circumglobal teleconnection over the Northern Hemisphere during boreal summer.

The warming of the Indian Ocean may act as a source of heating that can be exchanged between the ocean and the overlying atmosphere. In addition, the Indian Ocean remains anomalously warm for several of months after the peak of El Niño. In other words, while El Niño generally peaks at the end of austral spring and summer, the Indian Ocean remains anomalously warm until the following austral winter, when the Pacific warm events start to dissipate (Fig. 2a). Therefore, the IOBW can, in turn, feed back onto the atmosphere, inducing a delayed influence on regional climate. For instance, Xie et al. (2009) associated the IOBW with a “capacitor” in the sense that the Indian Ocean warms when El Niño matures (“charging the capacitor”) and exerts a delayed effect on the northwestern Pacific climate after the El Niño-related anomalies dissipate (“discharging the capacitor”).

A recent study by Taschetto et al. (2011) has shown that the Indian Ocean basin-wide warming tends to reinforce and prolong the dry conditions caused by El Niño over northwestern Australia from January to March. Following up Taschetto et al. (2011), we examine here the influence of the IOBW on a different region also largely affected by El Niño conditions.

South America is one of the continental regions around the world that is directly influenced by ENSO (Ropelewski and Halpert 1989). Several studies have documented its impacts on South American rainfall (Aceituno 1988; Grimm et al. 1998, 2000; Uvo et al. 1998; Diaz et al. 1998; Pezzi and Cavalcanti 2001; Coelho et al. 2002; Souza and Ambrizzi 2002; Taschetto and Wainer 2008; among others). Findings of these works indicate that, in general, the warm phase of ENSO influences the climate of South America over several regions including the west section (Peru and Ecuador), the south-southeast area (southern Brazil, Uruguay and Argentina) and the north and northeast parts of the continent (Amazonia and Northeast Brazil).

The Northeast Brazil is a densely populated region, inhabited by more than one quarter of the total country's population. Its economy, primarily based on agriculture,

cattle production and tourism, is dependent on the patterns of rainfall over the region. The northern sector of Northeast Brazil relies on the seasonal migration of the Atlantic Inter-Tropical Convergence Zone (ITCZ) to receive rain. The rainy season over the semi-arid Northeast Brazil occurs from March to May, when the Atlantic ITCZ reaches its most southward position (Uvo et al. 1998). The rainy season, however, experiences very large interannual variability, reaching 40% of the mean (Uvo et al. 1998). The southern sector of Northeast Brazil receives most of the annual rainfall during austral summer. As such, a better knowledge of the mechanisms modulating precipitation variability over Northeast Brazil would possibly improve rainfall predictions over the region.

The eastward shift of anomalously warm waters associated with El Niño events induces changes in the Walker circulation, such that ascending air occurs in the eastern tropical Pacific and descending motion over Northeast Brazil. The anomalous subsidence caused by the Walker circulation anomaly suppresses convection, inhibits the formation of clouds and thus decreases rainfall over that region. In addition to the Walker circulation anomaly, ENSO can also significantly modulate rainfall across the South American subtropics via the Pacific-South American pattern (PSA; Karoly 1989; Grimm 2003). Generally, the anomalous circulation associated with the PSA tends to strengthen the South American low level jet that transports moisture from the Amazon basin to the subtropics, thus reducing rainfall over eastern Brazil and enhancing it over La Plata (Herdies et al. 2002).

In contrast to the well-documented impacts of ENSO, the effects of the Indian Ocean variability onto South American climate is less understood. Previous studies show that, during austral spring, the IOD can remotely affect the atmospheric circulation over South America (Saji et al. 2005) leading to a significant impact on precipitation (Chan et al. 2008). Drumond and Ambrizzi (2008) reported that warm SST anomalies in the subtropical Indian Ocean give rise to a South American teleconnection pattern, which potentially induces changes onto the circulation and rainfall over the continent during austral summer. None of these previous studies, however, explore a possible connection between the IOBW and the South American climate.

In this study, we investigate the impact of the IOBW on atmospheric circulation and precipitation over South America. In the next section, the observed and reanalysis data as well as the numerical experiments are described. Section 3 presents the results and discusses the mechanisms involved in the link between the Indian Ocean SST and South American climate. Finally, Sect. 4 summarizes the main conclusions of this work.

2 Data and methods

2.1 Observational data and reanalysis

The precipitation dataset used in this study is from the Global Precipitation Climatology Center (GPCC). This dataset is based on rain gauge measurements interpolated over land areas, using a spatial objective analysis. The GPCC is a monthly data set arranged on a 2.5° latitude by 2.5° longitude grid and covers the period 1951–2004 (Rudolf et al. 1994; Beck et al. 2005). The SST field is based on the global sea ice and SST data from the Hadley Centre (HadISST1). The HadISST1 is disposed on a $1^\circ \times 1^\circ$ grid and is available for 1870 to present. Details of this SST dataset can be found in Rayner et al. (2003).

The indices for the Indian and Pacific modes of variability are derived from the HadISST1. The Niño3 index is calculated as the averaged SST anomalies in the eastern Pacific between 90°W – 150°W and 5°S – 5°N . The IOD index is calculated as in Saji et al. (1999), i.e. the difference between the SST anomaly in the western Indian Ocean (50°E – 70°E , 10°S – 10°N) and the southeast region (90°E – 110°E , 10°S – 0°). The IOBW index is calculated as the leading principal component of the tropical Indian Ocean SST anomalies shown in Fig. 1b.

We also use the National Center for Environmental Prediction (NCEP)—National Center for Atmospheric Research (NCAR) Reanalysis (Kalnay et al. 1996) to analyse atmospheric fields where observations are limited, such as vertical velocity, streamfunction and horizontal winds at low (850 hPa) and high (200 hPa) troposphere.

For consistency purposes, all datasets are analyzed for the same period as the GPCC, i.e. from 1951 to 2004. The primarily focus of the analysis is the interannual variability, and as such all data were linearly detrended.

2.2 The model and the numerical experiments

The Community Atmospheric Model (CAM3) from the NCAR is used in this study. The CAM3 has a T42 spectral truncation in the horizontal (i.e. approximately $2.8^\circ \times 2.8^\circ$ in longitude and latitude) and 26 levels in a hybrid vertical system that combines a terrain-following sigma coordinate at the bottom surface with a pressure-level coordinate at the top of the model. A complete description of CAM3 can be found in Collins et al. (2004).

The numerical experiments consist of 5-member ensemble forced by prescribed SST from the HadISST over the following four domains: (1) the Global Oceans; (2) the tropical Indian Ocean north of 30°S ; (3) the tropical Pacific Ocean between 30°N and 30°S ; and, (4) the Indo-Pacific region between the latitude band of 30°S and 30°N and bounded by Africa and South America in longitude. The

Global Oceans experiment allows us to analyse the performance of the model compared to observations given the limitation that there is no feedback to the ocean. The atmospheric response to the IOBW can be examined with the Indian Ocean experiment as there are no other modes of variability forcing the model in this simulation. Finally, the Pacific Ocean and Indo-Pacific experiments provide an estimate of the extent to which the South American rainfall and circulation change in the presence of ENSO. This latter experiment is motivated by the co-occurrence of El Niño events with the Indian Ocean warming.

The prescribed SST contains all observed variations, i.e. month-by-month to multidecadal variability plus trends. In order to minimize spurious effects from the edges of the boundary forcing, the SST anomalies are linearly damped in a 10° band of latitude to their climatological values at 30°S . Monthly-varying climatological mean SST based on the period 1949–2006 are assigned outside the Indian Ocean domain.

Each ensemble member is integrated from January 1949 to August 2009. However, in order to compare with the observational results, the ensemble mean is analyzed for the same period as the GPCC dataset (i.e. 1951–2004).

The integrations differ from each other by slightly distinct initial conditions of the atmosphere. This gives an estimate of the internal variability of the climate system. The ensemble mean is used here as the best representation of the simulated climate system to the SST forcing by the CAM3. Averaging the ensemble members reduces the internal atmospheric variability (considered noise for this study) and highlights the external signal forced by the underlying SST.

3 Results

3.1 Impacts on observed rainfall

The relationship between the IOBW and South American precipitation is initially assessed via correlation analysis, as shown in Fig. 3. Overall, the monthly correlations tend to be negative in the north and positive in the south, exhibiting a dipole-like pattern over the continent during certain months (e.g. November). The negative coefficients over the north and northeast regions of South America are particularly interesting from March to May (MAM) for two reasons. Firstly, the Northeast Brazil is considered to be one of the regions on the globe that has a strong link with warm events in the equatorial Pacific (e.g. Ambrizzi et al. 2004). However, there are no previous studies that associate a dynamical link between the Indian Ocean and the Northeast Brazil. The rainy season in the northern sector of Northeast Brazil occurs in MAM, thus a better knowledge

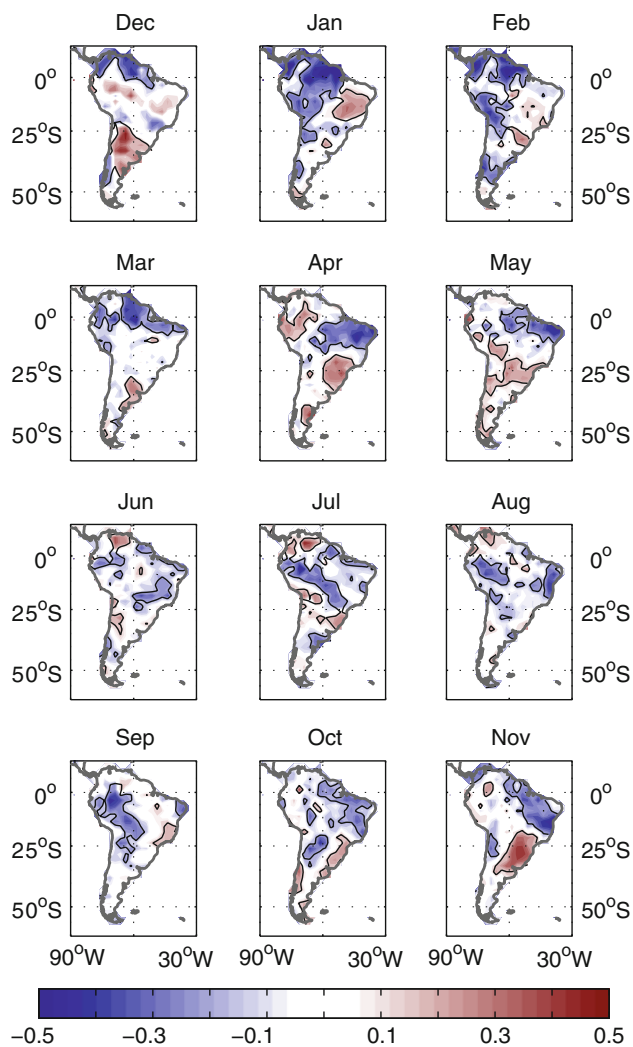


Fig. 3 Monthly correlations between South American precipitation and the Indian Ocean basin-wide warming. The areas within the thin black line are significant at the 0.1 level

of the mechanisms affecting Northeast Brazil would possibly improve rainfall prediction for the region. Secondly, it is during the austral autumn that El Niño dissipates (Spencer 2004; Fig. 2a, black line), so its influence on climate is expected to be weaker than during other seasons. As such, the ability for the IOBW to modulate rainfall in the region would be enhanced.

The results in Fig. 3 illustrate a statistical dependence between the IOBW and South American rainfall. The IOBW is associated with below-normal rainfall over Northeast Brazil during MAM. With the tropical Indian Ocean slightly warmed after the peak of El Niño events, it is likely that the anomalous descending motion (initiated by ENSO warm events) intensifies and/or persists over the region.

To focus on the northeastern South America (NESA) region, we average the rainfall anomalies over the area 0°S – 15°S , 60°W – 34°W , coinciding with the regions of

negative correlations observed throughout all months. This area covers the Northeast Brazil and parts of the North and Central regions of the country. Figure 4 depicts the annual cycle of correlations between the average rainfall anomalies over the NESA region and the IOBW and Niño3 Indices. The NESA rainfall is significantly correlated with Niño3 from March to August. It is interesting to note that during MAM, the IOBW \times NESA correlations become significant (Fig. 3). As the IOBW is strongly connected to El Niño events, one could argue that this result is contaminated by the effect of ENSO warm episodes. Indeed, the significant correlation coefficients of the NESA rainfall and the IOBW can reflect a mixed influence of both oceans. Separating the effect of each oceanic basin is a challenging task, as these episodes co-occur. In order to examine the relative influence of each warm event onto the NESA precipitation, we use partial correlations where the signal of the Niño3 index is first removed from the IOBW and NESA rainfall by linear regression. Figure 5 shows the remaining IOBW signal over South America during MAM. Despite smaller coefficients, the IOBW reveals significant correlations over South America after the exclusion of ENSO's influence.

Caution should be taken when partial correlation analysis is performed onto two phenomena that are dynamically linked. The partial correlation/regression used here assumes that there is a linear relationship between the events. In nature, however, the impact of the Pacific onto the Indian Ocean can have a nonlinear component. For that reason, we also use an AGCM as another method to separate the relative effect of the Indian Ocean onto South

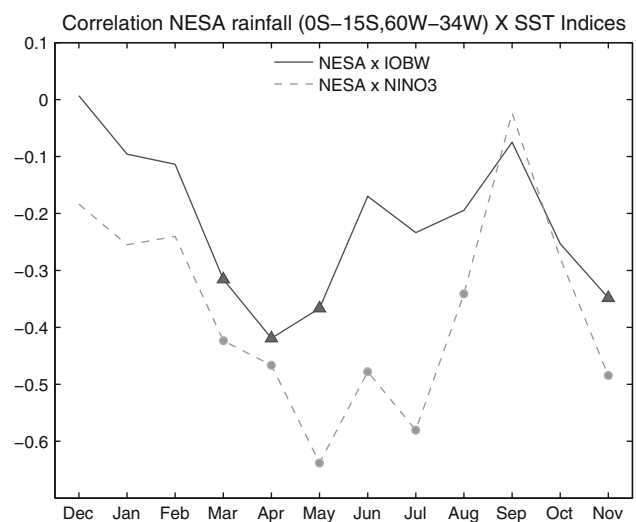


Fig. 4 Month-by-month correlations between precipitation in northeastern South America between 0°S – 15°S , 60°W – 34°W and the IOBW (dark gray line) and the Niño3 index (light-dashed gray). Symbols indicate correlations significant at the 0.05 level

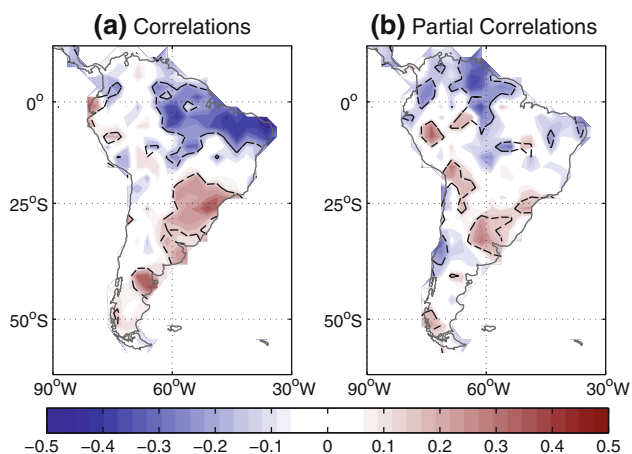


Fig. 5 Partial correlations between South American MAM rainfall and the IOBW, excluding the influence of Niño3 index. Areas within the *thin black line* represent correlations significant at the 0.1 level

American rainfall. The great advantage of using numerical experiments is that we can run the model using one type of forcing while excluding the other. The Indian Ocean experiment used in this study does not contain the forcing of the Pacific SST variability, although variability in the Indian Ocean SST anomalies may reflect the ENSO signal.

3.2 Simulated rainfall

In order to investigate the mechanisms associated with the impact of IOBW on South American climate, we first assess the extent to which the observed correlation patterns are captured by the NCAR CAM3 model. Figure 6 shows the month-to-month correlations between the IOBW and the simulated South American rainfall from the Global Ocean experiment. In general, the model well-simulates the dipole pattern with negative correlations in the north of the continent and positive correlations in the south. However, it is clear that the model tends to overestimate the correlation coefficients relative to observations. It is likely that the model overestimates the forced component of the atmospheric response to the imposed SST forcing. Yu and Mechoso (1999) discuss that the lack of feedback with the ocean tends to simulate an excessive latent heat flux in AGCM simulations, particularly over the tropics, which can, in turn, overestimate the atmospheric circulation response to the boundary forcing. Although a correct representation of precipitation in AGCMs can be difficult (due to the diversity of model parameterizations, model resolution, etc.), South American rainfall has been shown to be generally more reproducible by AGCMs when compared to the South-Asia and Australian monsoons (Zhou et al. 2008). Taschetto and Wainer (2008) examined the reliability of the NCAR CAM3 model in representing the climatological precipitation over South America and found

a satisfactory consistency in the intensity and seasonality relative to the observed patterns.

It is also noteworthy that we use an ensemble mean instead of a single simulation for the correlation analysis. The ensemble mean smoothes variations associated with internal variability while also highlighting the external signal related to the SST forcing. In this way, the correlation coefficients with the ensemble mean are slightly enhanced compared to those with individual members.

Despite overestimating correlation maps, the NCAR CAM3 appears to provide a reasonable simulation of the seasonality of the relationship between the IOBW and rainfall, with correlations decreasing considerably during austral winter and increasing from spring to autumn. In addition, the model seems to reasonably capture the dipole structure seen in observations from November to May. The model simulates a reduction in rainfall over northern South America and an increase in precipitation in the southeast

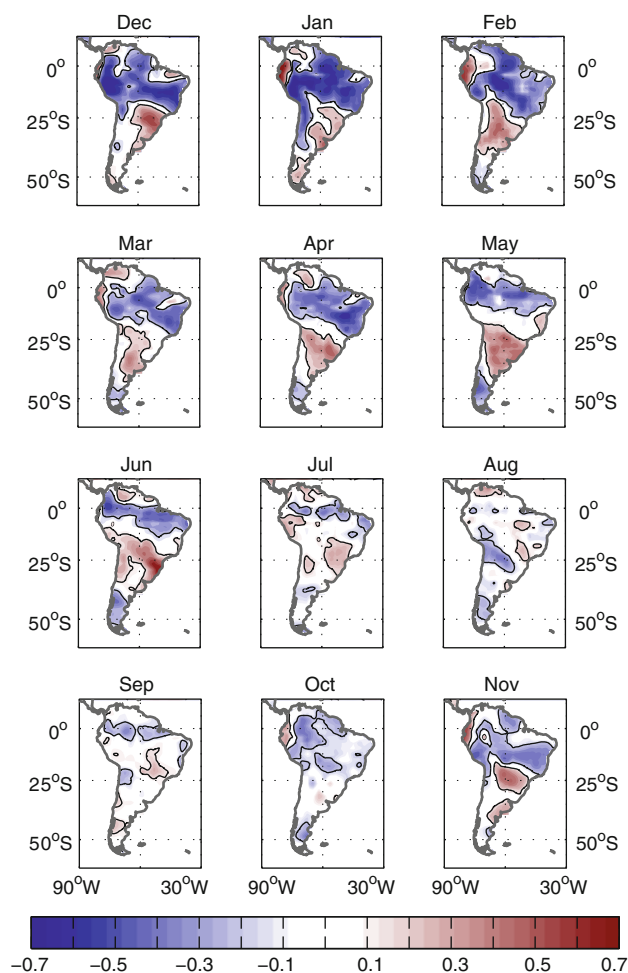


Fig. 6 Month-by-month correlations between the IOBW and simulated South American rainfall from the Global Ocean experiment. Areas within the *thin black line* represent correlations significant at the 0.1 level

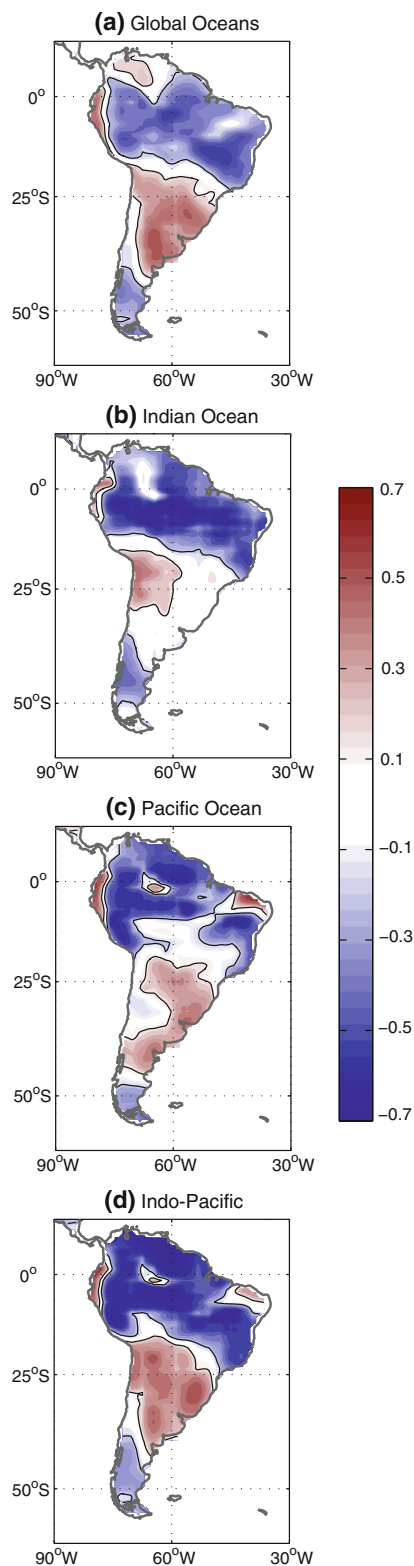


Fig. 7 Correlations between the IOBW and the simulated South American precipitation for **a** the Global Oceans, **b** Indian Ocean, **c** Pacific Ocean and **d** Indo-Pacific experiments. Areas within the *thin black line* represent correlations significant at the 0.1 level

when the tropical Indian Ocean is anomalously warm. When SST anomalies are applied only in the Indian Ocean (i.e. in the Indian Ocean experiment), the simulated rainfall response resembles that of Fig. 6, but correlation coefficients are even stronger for all months (not shown).

In the analysis below, we focus on MAM when observed rainfall is significant over NESa (Fig. 4), coinciding with a weakened El Niño but active IOBW (Fig. 2a). Figure 7 shows the MAM correlations for all the experiments. A clear and strong dipole pattern is seen in the correlations between rainfall and IOBW. In the Global Ocean experiment (Fig. 7a), the IOBW index is associated with dry conditions over the Central, North and Northeast regions of Brazil, extending westward across Bolivia and Peru and over the southern tip of the continent. Wet conditions associated with IOBW are seen over Ecuador, Venezuela, South Brazil, Uruguay, Paraguay and northern Argentina. The experiment forced with the Indian Ocean SST anomalies only (Fig. 7b) reveals a similar pattern of correlations to that of the Global Ocean experiment, except for the area of positive correlations that is reduced and located west of 60°W. This indicates that the MAM rainfall signal over south Brazil and the La Plata region is more likely to be modulated by ENSO and other factors than by the IOBW. Indeed, the Pacific Ocean experiment (Fig. 7c) shows positive correlations over the La Plata region, but not as extensive in the west. The area with positive correlations simulated in the Global Oceans is recovered when both Indian and Pacific SST anomalies are considered in the experiment (Fig. 7d).

Interestingly, the northern sector of the Northeast Brazil reveals significant positive correlations in the Pacific Ocean experiment (Fig. 7c), a signal that remains in the Indo-Pacific experiment (Fig. 7d) but disappears in the Global Oceans and the Indian Ocean experiments (Fig. 7a, b). This suggests that the Indian Ocean, in conjunction with other factors (e.g. tropical Atlantic), can contribute to the below-average MAM precipitation over Northeast Brazil during El Niño years.

The strong link between the IOBW and the NESa rainfall is also evident in the annual cycle of correlations shown in Fig. 8. It reveals coefficients larger than 0.65 from March to May, which suggests that the IOBW contributes to over 40% of the explained variance of the NESa precipitation in the numerical experiment. As expected, correlations between the Niño3 index and the NESa rainfall are small during most of the year, except for January to March. The absence of the tropical Pacific Ocean in this experiment allows the Indian Ocean to perturb the global atmosphere and affect the NESa region without the influence of other remote factors.

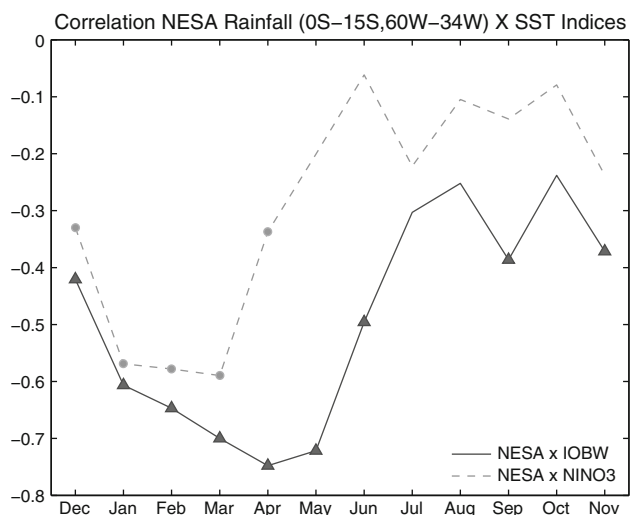


Fig. 8 Annual cycle of 3-months running mean correlation between the simulated precipitation in northeastern South America (0°S – 15°S , 60°W – 34°W) and the IOBW (dark gray line) and the Niño3 index (light-dashed gray). Symbols indicate correlations significant at the 0.05 level. Simulated rainfall from the Indian Ocean experiment

Observations and experiments shown so far support the idea that the IOBW holds a statistical link with the northeast South American precipitation. The mechanisms by which this connection exists are explored in the next section. Focus is placed on the austral autumn season when both observations and simulations show consistent signal to IOBW.

3.3 The mechanisms

To investigate the mechanisms by which the Indian Ocean warming affects precipitation over South America, we regress the vertical velocity anomalies meridionally averaged over 10°S – 10°N onto the IOBW index. Figure 9 exhibits the result for the reanalysis. In order to minimize the observed effects of the tropical Pacific forcing, we perform a partial regression on the reanalysis data with the Niño3 index removed. Negative (positive) values of vertical velocity indicate upward (downward) motion.

Figure 9a shows strong upward motion over the longitudes ranging from approximately 170°E to 80°W and subsidence over Indonesia, Africa and South America. When El Niño is linearly removed from the regressions, the magnitude of the vertical velocity anomaly is considerably reduced as seen in Fig. 9b. Despite ENSO being previously removed from the analysis, there still remains a clear signal over the tropical Pacific. The fact that the ENSO signal cannot be completely removed can be a consequence of two factors: (1) we use the Niño3 index as a proxy for ENSO, but El Niño events can reach far west in the equatorial Pacific; and, (2) we use linear regression to

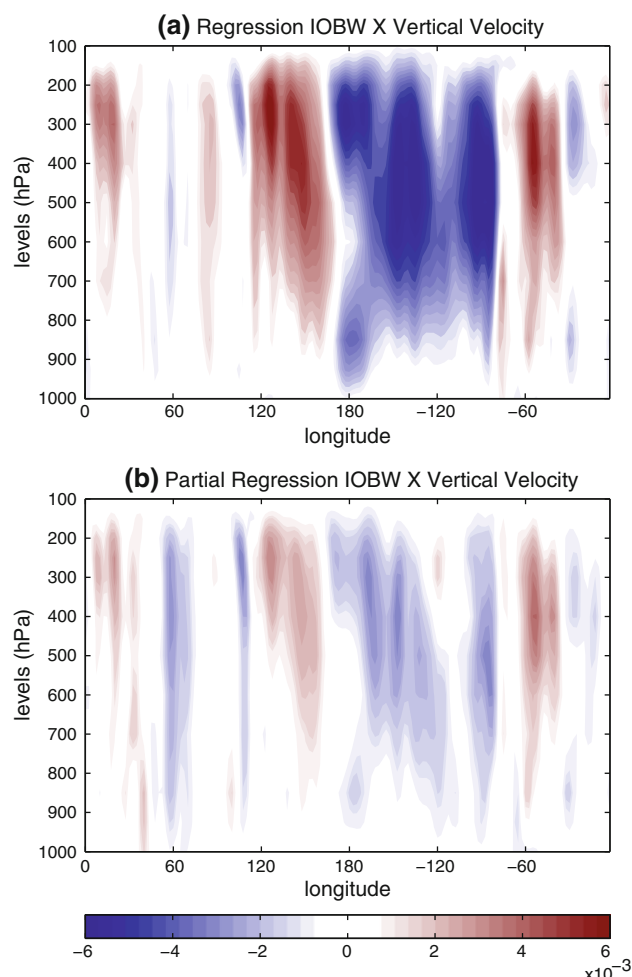


Fig. 9 **a** Partial regression of IOBW onto MAM vertical velocity (Pa s^{-1}) from NCEP/NCAR reanalysis. **b** Partial regression with ENSO signal excluded from (a)

remove ENSO's influence from the vertical velocity, however nonlinearities in this relationship may exist. Over the Indian Ocean longitudes, a weak but significant updraft occurs around 60°E (Fig. 9b). This weak updraft is likely to be a response of the underlying warm water that may reinforce subsidence over Africa and Indonesia.

The Indian Ocean experiment clearly shows upward motion from approximately 40°E to 120°E . Without the influence of the Pacific, strong upward motion is simulated over the tropical Indian Ocean and significant subsidence is located over the Maritime continent, Africa, Atlantic and South America (Fig. 10a). No signal is found over the Pacific Ocean, suggesting that the teleconnections with South America occur westward. The upward motion caused by the IOBW alters the vertical circulation generating subsidence over the tropical Atlantic and extending throughout South America in MAM. This anomalous circulation reduces the vertical motion, inhibits the formation

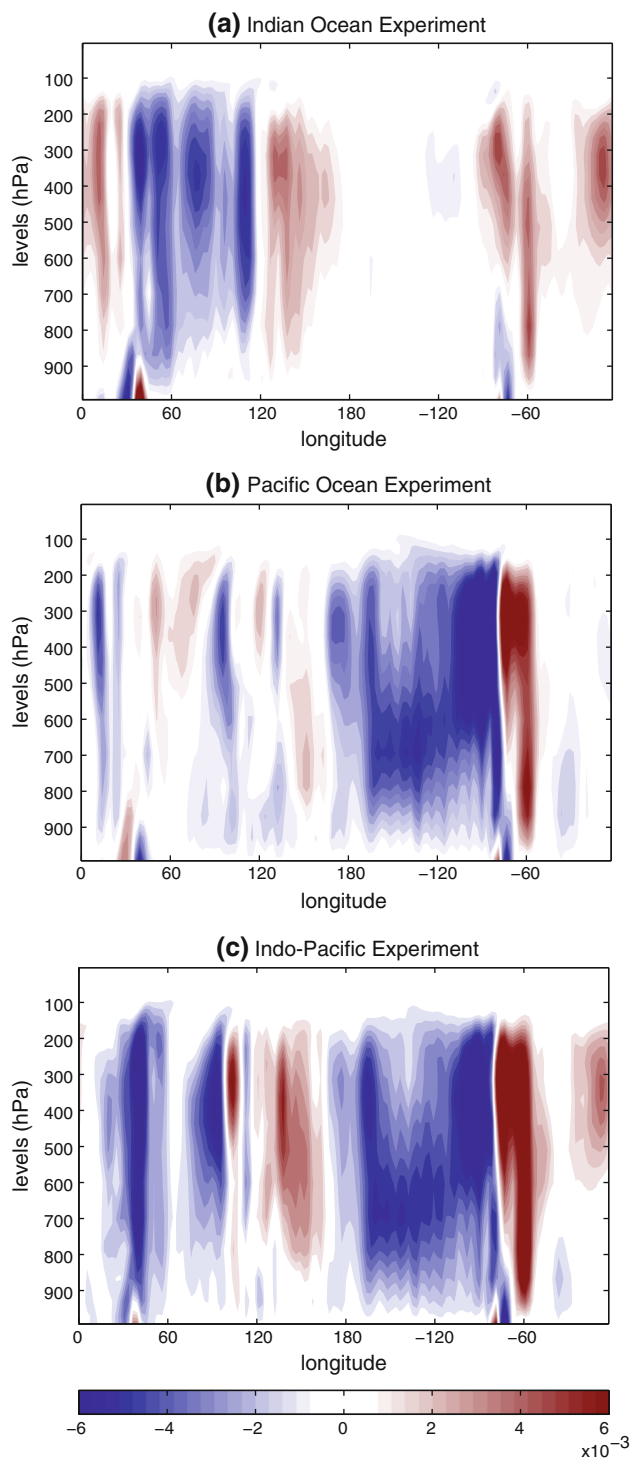


Fig. 10 Regression of IOBW onto MAM vertical velocity (Pa s^{-1}) for **a** the Indian Ocean experiment, **b** the Pacific Ocean experiment and **c** the Indo-Pacific experiment

of clouds, and consequently leads to less precipitation over tropical South America.

The experiment forced with the Pacific SST anomalies only exhibits intense ascending motion over the El Niño

longitudes and strong downward motion over South America (Fig. 10b). A less defined structure is seen over Indonesia and the Indian Ocean. Contrasting with the Indian Ocean experiment, Fig. 10b reveals an updraft over the African longitudes and no signal evident in the tropical Atlantic. The vertical velocity anomalies simulated in the Indo-Pacific experiment (Fig. 10c) seem to be a linear combination of both oceans. It exhibits strong upward motion in the tropical Pacific and Indian Ocean and downward motion over Indonesia, Atlantic Ocean and South America.

Figure 11 provides more evidence to support this climate process; it shows the response of the IOBW onto the simulated MAM velocity potential anomalies at 200hPa. Negative (positive) anomalies of velocity potential represent areas of divergent (convergent) flow at upper levels of the atmosphere. For the Indian Ocean experiment (Fig. 11a), strong divergent flow is seen over that basin and, by conservation of mass, convergence occurs at the upper troposphere over the Atlantic Ocean, Central America and northern South America. Consistent with the anomalous vertical velocity field of Fig. 10a, no signal is seen over the Pacific Ocean. This suggests that a dynamical teleconnection occurs from the IOBW to South America via a compensatory subsidence through the west.

For the Pacific Ocean experiment (Fig. 11b), the velocity potential anomalies regressed onto the IOBW depict a classical El Niño signature with a clear Walker circulation anomaly. Divergent flow is located at the upper troposphere over the eastern Pacific with a consequent convergence over the Maritime continent. Interestingly, the simulated anomalies over the Indian Ocean and Africa oppose those from the Indian Ocean experiment. In addition, no signal is virtually seen over the equatorial Atlantic.

Similar to the simulated vertical velocity anomalies, the velocity potential field of the Indo-Pacific experiment appears to be a linear combination of both tropical ocean basins (Fig. 11c). The area of ascending motion is slightly reduced in spatial extent and weakened over the Indian Ocean and eastern Africa compared to Fig. 11a. Relative to the Pacific Ocean experiment, the center of the anomalously positive velocity potential over Australia shifts eastwards and intensifies over Indonesia and northwestern Pacific, concentrating the anomalies in a traditional “horseshoe” that is characteristic of El Niño events. The positive velocity potential over the Atlantic Ocean and northeastern South America simulated in the Indo-Pacific experiment seems to be a response of the IOBW while the intensification of the anomalies over Venezuela represents a combination of both Indian and Pacific Ocean SST variability. The South American rainfall response to the IOBW occurs through the anomalous Walker circulation (Figs. 10a, 11a). The Indian Ocean SST anomalies perturb

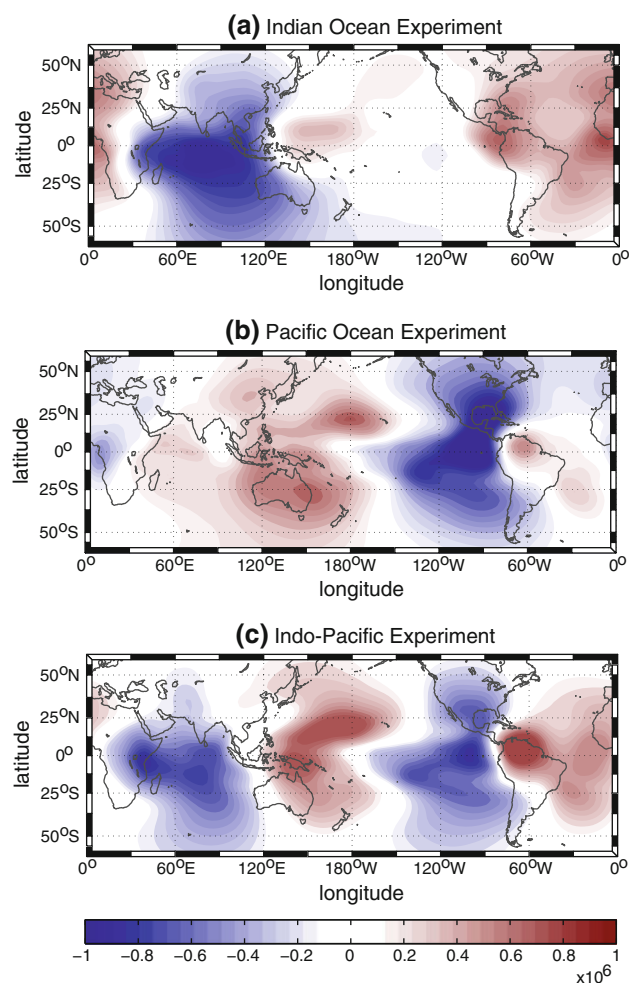


Fig. 11 Regression of IOBW onto the simulated velocity potential ($\text{m}^2 \text{s}^{-1}$) at 200 hPa for **a** the Indian Ocean experiment, **b** the Pacific Ocean experiment and **c** the Indo-Pacific experiment

the overlying atmosphere via changes in air-sea heat fluxes and low-level wind convergence, which, in turn, induces upward motion and, by continuity, descending motion over South America.

Figure 12 depicts the observed asymmetric streamfunction anomalies at 200 and 850 hPa partially regressed onto the IOBW. In the Southern Hemisphere, negative values of the zonally asymmetric streamfunction represent anticyclones and ridges. Overall, the regression fields show a baroclinic response in the tropical latitudes and a barotropic response in the southern subtropics. The partial regressions show a weaker signal of the IOBW over the Indian Ocean than the regression analysis (not shown). This happens because of the co-occurrence of the IOBW and El Niño and the large correlation between these phenomena. When the Niño3 index is linearly removed from the analysis, the 850 hPa anomalies over the western tropical Indian Ocean and the eastern tropical Pacific are virtually eliminated (Fig. 12b). However, an El Niño

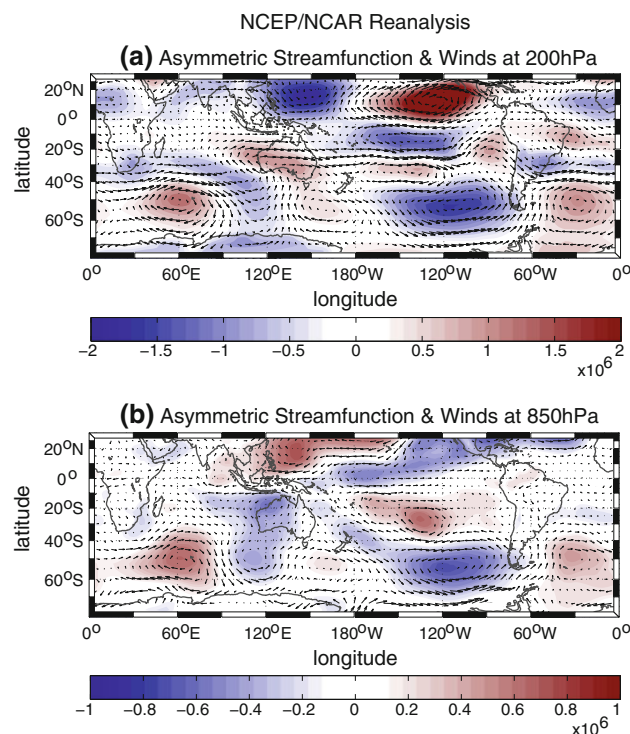


Fig. 12 Partial regression of the IOBW onto MAM asymmetric streamfunction ($\text{m}^2 \text{s}^{-1}$) and horizontal winds (m s^{-1}) at **a** 200 hPa and **b** 850 hPa from NCEP/NCAR reanalysis. Maximum vector length is 4 and 1 m/s, respectively

signature remains over the central and western tropical Pacific (despite smaller magnitudes). Over South America, weak northeasterly anomalies (Fig. 12b) enhance the South American low level jet, transporting moisture from tropical latitudes to the subtropics and favoring precipitation over La Plata (Fig. 5). Additionally, a remote response in the southern subtropics is manifested as a stationary Rossby wave-train with anomalous anticyclone in the southeastern Pacific and cyclonic circulation anomalies in the Indian and Atlantic sectors.

Figure 13 presents the atmospheric response simulated by the Indian Ocean experiment. A strong baroclinic signal is evident in the Indian Ocean as a response to the underlying warm waters from the IOBW. Figure 13 also shows that the wave-train feature in the southern subtropics is reproduced by the asymmetric streamfunction and wind anomalies simulated in the Indian Ocean experiment. A pair of cyclonic-anticyclonic anomalies associated with the IOBW is located in the Indian sector and south of Australia. In addition, a barotropic anticyclonic anomaly is found in the southeastern Pacific around 50°S, 90°W and a cyclonic anomaly in the South Atlantic extratropics. The observed cyclonic circulation anomalies in the south Indian and Atlantic Oceans are well captured by the model (compare Figs. 12b, 13b). The extratropical anticyclonic anomaly west off South

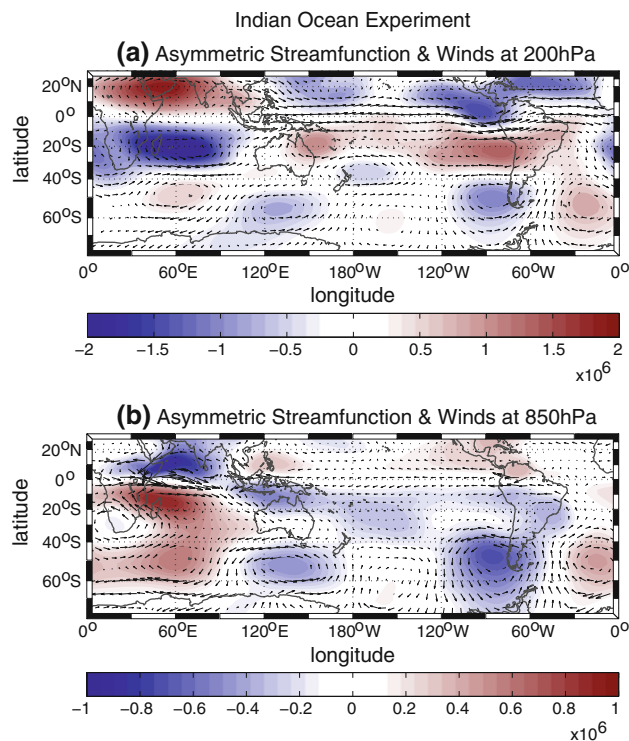


Fig. 13 Regression of the IOBW onto MAM asymmetric streamfunction ($\text{m}^2 \text{s}^{-1}$) and horizontal winds (m s^{-1}) at **a** 200 hPa and **b** 850 hPa for the Indian Ocean experiment. Maximum vector length is 3 and 2 m/s, respectively

America, however, does not extend beyond 120°W as observed in the reanalysis.

The simulated atmospheric response in the Pacific Ocean experiment, shown in Fig. 14, reveals a classical El Niño signature. The warm SST anomalies in the eastern Pacific perturb the overlying atmosphere via changes in air-sea heat fluxes and low-level wind convergence (Fig. 14b), which in turn induces upward motion (Fig. 10b). The anomalous vertical velocity over the underlying warm waters increases the moist convection and latent heat release, generating anomalous diabatic heating in the troposphere. Diabatic heating can give rise to disturbances in the upper troposphere, leading to propagation of equatorially trapped waves as in the Gill-Matsuno theory (Matsuno 1966; Gill 1980). The Gill-Matsuno mechanism manifests as a pair of anticyclones symmetric about the equator, clearly seen in the Pacific Ocean experiment (Fig. 14a).

When the model is forced by both Indian and Pacific Ocean SST variability (Fig. 15), the Gill-Matsuno response to El Niño (represented by the quadrupole anomaly in the eastern Pacific and South America) weakens slightly, as does the baroclinic signal over the tropical Indian Ocean. The wave-train feature is better defined in the Indian Ocean experiment than in the Pacific only experiment, which suggests the potential role of the IOBW in modulating the

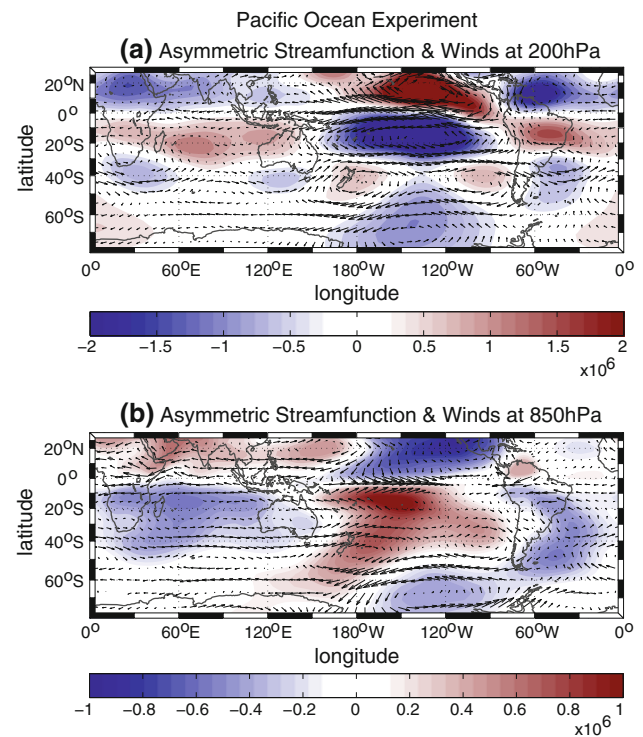


Fig. 14 Regression of the IOBW onto MAM asymmetric streamfunction ($\text{m}^2 \text{s}^{-1}$) and horizontal winds (m s^{-1}) at **a** 200 hPa and **b** 850 hPa for the Pacific Ocean experiment. Maximum vector length is 4 and 2 m/s, respectively

extratropical teleconnections to South America during El Niño events. The extratropical anticyclone over south-eastern Pacific becomes more elongated (Fig. 15b), resembling the observed feature in the reanalysis, although the entire wave-train pattern does not seem to improve.

For South America, the response to both Indian and Pacific Ocean together appears to be non-linear. The Indo-Pacific experiment simulates an elongated band of negative streamfunction anomalies associated with a cyclonic circulation in the lower troposphere over the South Atlantic Convergence Zone (SACZ; Fig. 15b). The anomalous winds north of this feature enhance the easterlies and induce an onshore flow from the Atlantic Ocean to the Northeast Brazil. These winds advect moisture to the continent causing the positive rainfall anomaly over the northern sector of the country, as detected by correlations pattern in Fig. 7d. The anomalous easterlies are deflected to the south, geostrophically following the band of negative streamfunction anomalies. This strengthens the South American low-level jet (Fig. 15b), possibly enhancing the moisture transport from the Amazon Basin to southern South America, generating positive rainfall to the region (positive precipitation correlation with the IOBW in Fig. 7d). This band of negative streamfunction anomalies over the SACZ region is also present in the Pacific Ocean

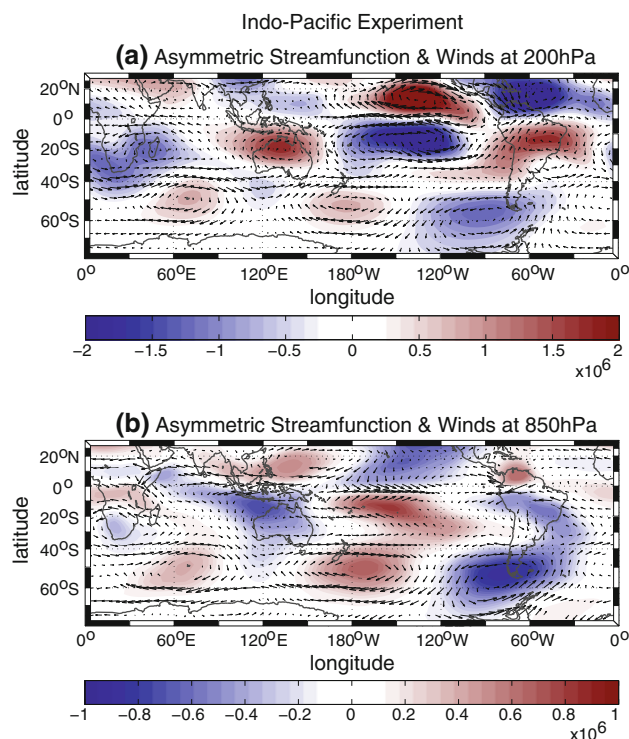


Fig. 15 Regression of the IOBW onto MAM asymmetric streamfunction ($\text{m}^2 \text{s}^{-1}$) and horizontal winds (m s^{-1}) at **a** 200 hPa and **b** 850 hPa for the Indo-Pacific experiment. Maximum vector length is 4 and 2 m/s, respectively

experiment, but a less elongated feature is simulated in the Indian Ocean experiment. As a consequence, the Indian Ocean experiment simulates northerly to northeasterly wind anomalies over central South America that confine the moisture transport and wet conditions to the west of the continent (see correlation pattern in Fig. 7b).

Saji et al. (2005) and Chan et al. (2008) have reported a similar teleconnection from the mid-latitude Indian Ocean during IOD events in SON. They show that this teleconnection leads to alterations in atmospheric circulation that manifests as a dipole signal in precipitation over subtropical South America. In addition, Drumond and Ambrizzi (2008) have described a similar wave-train teleconnection from the subtropical Indian Ocean to South America during December to February. Here we show that this mechanism can also happen during MAM, however the teleconnections from the IOBW to South America is such that the wet conditions are confined to the western region of the continent. Only when the Pacific is considered in conjunction with the Indian Ocean SST anomalies that wet conditions occur over the La Plata region, and the entire dipole rainfall pattern in South America is closely simulated to that in the Global Oceans. In general, extratropical teleconnections are more intense during the winter hemisphere due to the presence of a stronger subtropical jet, which acts as a

wave-guide for these kinds of disturbances. Therefore, a relatively weak IOD event (that peaks in September) is more likely to perturb the southern extratropics than an IOBW (that occurs during austral summer-autumn). On the other hand, Lee et al. (2009) demonstrate that stationary Rossby waves can be still excited in the summer hemisphere if the heating source is located in the vicinity of the jet. As the IOBW can reach higher southern latitudes than the warm SST anomalies associated with IOD events, it may also favour a significant wave-train teleconnection propagating over the southern mid-latitudes, as illustrated in Fig. 13.

4 Conclusions

In this study, we investigate the teleconnections between the tropical Indian Ocean basin-wide warming and the atmospheric circulation and precipitation over South America. A few studies have reported a wave-train teleconnection pattern from the Indian Ocean Dipole events to South American subtropics (Saji et al. 2005) with potential effects on rainfall variability over La Plata (Chan et al. 2008). However, less attention has been given to the impacts of the Indian Ocean basin-wide warming pattern that co-occur with El Niño events. As far as we are aware, there is only one study that addresses a possible effect from the Indian Ocean warming onto South American climate, i.e. Drumond and Ambrizzi (2008). Here we show that, despite being a remote response to El Niño events, the IOBW has the potential to feed back onto the atmosphere and induce tropical and extratropical teleconnections to South America.

Separating the effects of the Pacific and Indian Oceans is a difficult task, as non-linearities can arise from the interactions between these two ocean basins. An attempt is made here using partial regressions onto observations and reanalysis data. However, caution should be taken when interpreting these analyses as ENSO and the IOBW are dynamically connected. A second approach is thus used with a multidecadal ensemble from the NCAR CAM3 model forced by prescribed SST across the Indian Ocean only and climatology everywhere else. In this way, the SST variability is eliminated from the Pacific Ocean. At the same time, the atmospheric circulation responds to a single ocean basin, i.e. the Indian Ocean. In addition, an experiment forced by the tropical Pacific SST anomalies and another by the Indo-Pacific variability are used to assess how the IOBW teleconnections are affected in the presence of El Niño.

Results from observations, reanalysis and simulations provide evidence that South American rainfall can be modulated by Indian Ocean SST variability via remote

mechanisms. The tropical connection between the IOBW and the distant continent occurs via an anomalous Walker circulation. The simulated vertical velocity, velocity potential and asymmetric streamfunction anomaly fields for the Indian Ocean experiment suggest that the IOBW induces anomalous ascending motion over the warm waters that, by continuity, descends over Australia and to the west over Africa, the Atlantic Ocean and South America. Therefore, the tropical connection from the Indian Ocean to South America produces anomalous subsidence over the northeast of the continent that, in turn, reduces convection, cloud formation, and precipitation, causing anomalous dry conditions for the region during MAM. The Pacific and combined Indian and Pacific experiments produce strong subsidence located over Venezuela, while the Indian Ocean simulates subsidence over the tropical Atlantic and Northeast Brazil.

In the subtropics, analysis of the observed La Plata rainfall reveals significant correlations with the IOBW during MAM. An anticyclonic circulation is located over South America, inducing an offshore flow over the La Plata basin. This flow strengthens the South American low-level jet and consequently enhances the transport of moisture to the subtropics over the continent (Silva and Ambrizzi 2009). The result is an increase in rainfall over the South American subtropics. This anticyclone is simulated in all experiments, although the elongated anomaly in the Pacific and Indo-Pacific experiments tend to better reproduce the location of enhanced rainfall observed over the La Plata region. However, it is a combination of these ocean basins that generates the entire pattern of positive precipitation over central-south South America as simulated in the Global Oceans experiment.

The reanalysis also shows a mid-latitude stationary Rossby wave-train pattern associated with the IOBW. The Indian Ocean experiment reasonably well simulates the observed wave-train pattern, while the Pacific experiment tends to simulate a more zonal signal over the extratropics. The experiment forced by the combination of Pacific and Indian Ocean SST anomalies does not seem to improve the simulation of the observed wave-train feature. This suggests that the Indian Ocean, possibly in conjunction with other factors not considered in this study (e.g. extratropical Pacific and Atlantic Ocean), has the potential to generate the observed teleconnection throughout South America.

In summary, the IOBW has the potential to affect the remote circulation and modulate rainfall over South America via tropical and extratropical teleconnections. The co-occurrence of the Indian Ocean warming with the Pacific warming suggests that the IOBW enhances and prolongs the typical response from El Niño events over South America throughout austral autumn. This influence can have important implications for rainfall forecasting over South America.

Acknowledgments The authors are grateful to Dr. Laura Ciasto for her help in editing the manuscript. GPCC Precipitation data provided by the NOAA/OAR/ESRL PSD, Boulder, Colorado, USA, from their Web site at <http://www.esrl.noaa.gov/psd/>. The HadISST1 is available at the UK Meteorological Office, <http://www.badc.nerc.ac.uk/data/hadisst/>. Use of NCAR CAM3 model is gratefully acknowledged. The model simulations were run at the Australian Partnership for Advanced Computing National Facility. This research was supported by the Australian Research Council and the State of São Paulo Research Foundation (FAPESP). T. Ambrizzi has also received funding from CNPq (Brazilian National Council for Scientific and Technologic Development), and from the European Community's Seventh Framework Programme (FP7/2007–2013) under Grant Agreement No. 212492 (CLARIS LPB-A Europe-South America Network for Climate Change Assessment and Impact Studies in La Plata Basin).

References

- Aceituno P (1988) On the functioning of the Southern oscillation in the South America sector part I: surface climate. *Mon Wea Rev* 116:505–524
- Ambrizzi T, Souza EB, Pulwarty RS (2004) The Hadley and Walker regional circulations and associated ENSO impacts on the South American seasonal rainfall. In: Diaz HF, Bradley RS (eds) *The Hadley circulation: present, past and future*. Kluwer, Dordrecht, pp 203–238
- Annamalai H, Xie S-P, McCreary JP, Murtugudde R (2005) Impact of Indian Ocean sea surface temperature on developing El Niño. *J Clim* 18:302–319
- Ashok K, Guan Z, Yamagata T (2001) Impact of the Indian Ocean dipole on the relationship between the Indian monsoon rainfall and ENSO. *Geophys Res Lett* 28(23):4499–4502
- Baquero-Bernal A, Latif M, Legutke S (2002) On dipolelike variability of sea surface temperature in the tropical Indian Ocean. *J Clim* 15:1358–1368
- Beck C, Grieser J, Rudolf B (2005) A new monthly precipitation climatology for the global land areas for the period 1951 to 2000. DWD, *Klimastatusbericht KSB* 2004, pp 181–190
- Behera S, Luo J, Masson S, Rao S, Sakuma H (2006) A CGCM study on the interaction between IOD and ENSO. *J Clim* 19:1688–1705
- Cai W, Cowan T, Raupach M (2009) Positive Indian Ocean dipole events precondition southeast Australia bushfires. *Geophys Res Lett* 36:L19710. doi:10.1029/2009GL039902
- Chambers DP, Tapley BD, Stewart RH (1999) Anomalous warming in the Indian Ocean coincident with El Niño. *J Geophys Res* 104:3035–3047
- Chan S, Behera S, Yamagata T (2008) Indian Ocean dipole influence on South American rainfall. *Geophys Res Lett* 35(14): L14S12
- Clark CO, Webster PJ, Cole J (2003) Interdecadal variability of the relationship between the Indian Ocean zonal mode and East African coastal rainfall anomalies. *J Clim* 16(3):548–554
- Coelho CAS, Uvo CB, Ambrizzi T (2002) Exploring the impacts of the tropical Pacific SST on the precipitation patterns over South America during ENSO periods. *Theor Appl Climatol* 71:185–197
- Collins WD et al (2004) Description of the NCAR community atmosphere model (CAM 3.0). National Center for Atmospheric Research Rep. NCAR/TN-464 1 STR, p 226
- Drumond AR de M, Ambrizzi T (2008) The role of the South Indian and Pacific oceans in South American monsoon variability. *Theor Appl Climatol* 94:125–137

- Diaz AF, Studzinski CD, Mechoso CR (1998) Relationships between precipitation anomalies in Uruguay and Southern Brazil and sea surface temperature in Pacific and Atlantic Oceans. *J Clim* 11:251–271
- Dommenget D, Latif M (2002) A cautionary note on the interpretation of EOFs. *J Clim* 15:216–225
- Fischer A, Terray P, Delecluse P, Gualdi S, Guilyardi E (2005) Two independent triggers for the Indian Ocean dipole/zonal mode in a coupled GCM. *J Clim* 18:3428–3449
- Gill AE (1980) Some simple solutions for heat-induced tropical circulation. *Quart J Roy Meteor Soc* 106:447–462
- Grimm AM (2003) The El Niño impact on the summer monsoon in Brazil: regional processes versus remote influences. *J Clim* 16:263–280
- Grimm AM, Ferraz SET, Gomes J (1998) Precipitation anomalies in Southern Brazil associated with El Niño and La Niña events. *J Clim* 11:2863–2880
- Grimm AM, Barros VR, Doyle ME (2000) Climate variability in Southern South America associated with El Niño and La Niña events. *J Clim* 1:35–58
- Herdies DL, da Silva A, Silva Dias MAF, Nieto-Ferreira R (2002) Moisture budget of the bimodal pattern of the summer circulation over South America. *J Geophys Res* 107:8075–8088
- Kalnay E et al (1996) The NCEP/NCAR 40-years reanalysis project. *Bull Am Meteor Soc* 77:437–471
- Karoly DJ (1989) Southern Hemisphere circulation features associated with El-Niño Southern Oscillation. *J Clim* 2:1239–1252
- Klein SA, Soden B, Lau N-C (1999) Remote sea surface temperature variations during ENSO: evidence for a tropical atmospheric bridge. *J Clim* 12:917–932
- Lau N-C, Nath MJ (2003) Atmosphere-Ocean variations in the Indo-Pacific sector during ENSO episodes. *J Clim* 16:3–20
- Lee S-K, Wang C, Mapes BE (2009) A simple atmospheric model of the local and teleconnection responses to tropical heating anomalies. *J Clim* 22(2):272–284
- Matsuno T (1966) Quasi-geostrophic motions in the equatorial area. *J Meteor Soc Jpn* 44:25–43
- Pezzi LP, Cavalcanti IFA (2001) The relative importance of ENSO and tropical Atlantic sea surface temperature anomalies for seasonal precipitation over South America: a numerical study. *Clim Dyn* 17:205–212
- Rayner NA, Parker DE, Horton EB, Folland CK, Alexander LV, Rowell DP, Kent EC, Kaplan A (2003) Global analyses of sea surface temperature, sea ice, and night marine air temperature since the late nineteenth century. *J Geophys Res* 108(D14):4407. doi:10.1029/2002JD002670
- Ropelewski CF, Halpert MS (1989) Precipitation patterns associated with the high index phase of the Southern Oscillation. *J Clim* 2:268–284
- Rudolf B, Hauschild H, Rueth W, Schneider U (1994) Terrestrial precipitation analysis: operational method and required density of point measurements. In: Desbois M, Desalmond F (eds) *Global precipitations and climate change*, NATO ASI series I, vol 26. Springer, Berlin, pp 173–186
- Saji NH, Goswami BN, Vinayachandran PN, Yamagata T (1999) A dipole mode in the tropical Indian Ocean. *Nature* 401:360–363
- Saji NH, Ambrizzi T, Ferraz SET (2005) Indian Ocean dipole mode events and austral surface temperature anomalies. *Dyn Atmos Oceans* 39:87–102
- Schott FA, Xie S, McCreary JP (2009) Indian Ocean circulation and climate variability. *Rev Geophys* 47:RG1002
- Silva GAM, Ambrizzi T (2009) Summertime moisture transport over Southeastern South America and extratropical cyclones behavior during inter-El Niño events. *Theor Appl Climatol* 101:303–310
- Souza EB, Ambrizzi T (2002) ENSO impacts on the South American rainfall during 1980s: Hadley and Walker circulation. *Atmosfera* 15:105–120
- Spencer H (2004) Role of the atmosphere in seasonal phase locking of El Niño. *Geophys Res Lett* 31(24):L24104
- Taschetto AS, Wainer I (2008) The impact of the subtropical South Atlantic SST on South American precipitation. *Ann Geophys* 26(11):3457–3476
- Taschetto AS, Sen Gupta A, Hendon HH, Ummenhofer CC, England MH (2011) The relative contribution of Indian Ocean sea surface temperature anomalies on Australian summer rainfall during El Niño events. *J Clim* 24:3734–3747
- Ummenhofer CC, Sen Gupta A, England MH, Reason C (2009a) Contributions of Indian Ocean Sea surface temperatures to enhanced East African rainfall. *J Clim* 22(4):993–1013
- Ummenhofer CC, England MH, McIntosh PC, Meyers GA, Pook MJ, Risbey JS, Sen Gupta A, Taschetto AS (2009b) What causes southeast Australia's worst droughts? *Geophys Res Lett* 36:L04706. doi:10.1029/2008GL036801
- Uvo CRB, Repelli CA, Zebeak SE, Kushnir Y (1998) The relationships between tropical Pacific and Atlantic SST and northeast Brazil monthly precipitation. *J Clim* 11:551–562
- Xie S-P, Hu K, Hafner J, Tokinaga H, Du Y, Huang G, Sampe T (2009) Indian Ocean capacitor effect on Indo-Western Pacific climate during the summer following El Niño. *J Clim* 22:730–747
- Yang J, Liu Q, Liu Z, Wu L, Huang F (2009) Basin mode of Indian Ocean sea surface temperature and Northern Hemisphere circumglobal teleconnection. *Geophys Res Lett* 36:L19705
- Yu J-Y, Mechoso CR (1999) A discussion on the errors in the surface heat fluxes simulated by a coupled GCM. *J Clim* 12:416–426
- Zhou T, Yu R, Li H, Wang B (2008) Ocean forcing to changes in global monsoon precipitation over the recent half-century. *J Clim* 21:3833–3852